ORIGINAL ARTICLE

Chrysophanol exerts a protective effect against Aβ$_{25\text{-}35}$-induced Alzheimer's disease model through regulating the ROS/TXNIP/NLRP3 pathway

Meng Zhang[1] · Zhi-xian Ding[1] · Wei Huang[1] · Jing Luo[1] · Shu Ye[1] · Sheng-lin Hu[1] · Peng Zhou[1] · Biao Cai[1]

Abstract

Background The primary pathogenic factors of Alzheimer's disease (AD) have been identified as oxidative stress, inflammatory damage, and apoptosis. Chrysophanol (CHR) has a good neuroprotective effect on AD, however, the potential mechanism of CHR remains unclear.

Purpose In this study, we focused on the ROS/TXNIP/NLRP3 pathway to determine whether CHR regulates oxidative stress and neuroinflammation.

Methods D-galactose and Aβ$_{25\text{-}35}$ combination were used to build an in vivo model of AD, and the Y-maze test was used to evaluate the learning and memory function of rats. Morphological changes of neurons in the rat hippocampus were observed using hematoxylin and eosin (HE) staining. AD cell model was established by Aβ$_{25\text{-}35}$ in PC12 cells. The DCFH-DA test identified reactive oxygen species (ROS). The apoptosis rate was determined using Hoechst33258 and flow cytometry. In addition, the levels of MDA, LDH, T-SOD, CAT, and GSH in serum, cell, and cell culture supernatant were detected by colorimetric method. The protein and mRNA expressions of the targets were detected by Western blot and RT-PCR. Finally, molecular docking was used to further verify the in vivo and in vitro experimental results.

Results CHR could significantly improve learning and memory impairment, reduce hippocampal neuron damage, and reduce ROS production and apoptosis in AD rats. CHR could improve the survival rate, and reduce the oxidative stress and apoptosis in the AD cell model. Moreover, CHR significantly decreased the levels of MDA and LDH, and increased the activities of T-SOD, CAT, and GSH in the AD model. Mechanically, CHR significantly reduced the protein and mRNA expression of TXNIP, NLRP3, Caspase-1, IL-1β, and IL-18, and increase TRX.

Conclusions CHR exerts neuroprotective effects on the Aβ$_{25\text{-}35}$-induced AD model mainly by reducing oxidative stress and neuroinflammation, and the mechanism may be related to ROS/TXNIP/NLRP3 signaling pathway.

Keywords Chrysophanol · Alzheimer's disease · ROS · TXNIP · NLRP3 pathway · Oxidative stress · Neuroinflammation

Introduction

Alzheimer's disease (AD) is a prevalent central nervous degenerative disease characterized by progressive dementia. Cognitive impairment, memory impairment, and personality disorder are the most common clinical signs of AD (Insel et al. 2021). At present, there are acetylcholinesterase (AchE) inhibitors, *N*-methyl-D-aspartate receptor (NMDA) inhibitors, antioxidants, APOE, and β-amyloid protein production inhibitors, etc. (Se Thoe et al. 2021; Sharma et al. 2019), but there is no therapeutic drug that can completely cure AD. Despite the considerable efforts that have been made to tackle the disease, AD remains inevitable and incurable. The high failure rate of

Meng Zhang and Zhi-xian Ding contributed equally to this work.

✉ Peng Zhou
zhoupeng@ahtcm.edu.cn

✉ Biao Cai
caibiao@ahtcm.edu.cn

[1] Department of Integrated Traditional Chinese and Western Medicine, Key Laboratory of Xin'an Medicine (Anhui University of Chinese Medicine), Ministry of Education, Anhui University of Chinese Medicine, Hefei 230012, People's Republic of China

AD drug development was believed to be mainly due to our insufficient understanding of the complex pathological mechanisms (Ju and Tam 2022). Therefore, it is of great significance to clarify the pathogenesis of AD and find safe and effective drugs for the prevention and treatment of AD.

Inflammasomes have an important role in the innate immune system and can promote inflammatory responses and apoptosis, which can result in various forms of neurodegeneration. Nucleotide-binding domain and leucine-rich repeat protein 3 (NLRP3) inflammasome is one of the typical features of AD (Lahooti et al. 2021). Studies have found that oxidative stress injury is related to inflammation, which can further cause damage through oxidative stress. Thioredoxin interaction protein (TXNIP) as a member of the α-block protein superfamily, it can regulate and maintain the balance between the intracellular oxidation and antioxidant system (Ye et al. 2017), activate the NLRP3 inflammasome under the drive of oxidative stress (Kelley et al. 2019; Dai et al. 2022), and further activate the downstream pathway, leading to inflammatory reaction and nerve cell damage (Du et al. 2020; Lu et al. 2018).

Chinese medical herb rhubarb is the dried rhizomes and roots of the Rheum palmatum L., mainly including anthraquinones, bupropion, and anthocyanins has been widely applied for treating various inflammatory diseases (Gu et al. 2022). Chrysophanol (CHR), the main anthraquinone from rhubarb, has anti-myocardial ischemia, improving fat metabolism, anti-inflammatory, diuresis, anticancer, and neuroprotective effects (Lim et al. 2018; Su et al. 2020; Xie et al. 2019). Pharmacological studies showed that CHR binds to DNA in a manner similar to that of ethidium bromide, mitoxanone, and adriamycin, but it is not as potentially toxic as other drugs, and its drug binding saturation value is low. The results of the DNA synthesis test and hypoxanthine–guanine phosphoribosyl transferase test showed that the toxicity of CHR could be ignored (Yusuf et al. 2019). Zhang et al. found that the LD_{50} of CHR was 2.5 g/kg, and the high value showed that it was toxic only at high doses (Zhang et al. 2012). Lo et al. found that in the toxicity test of primary rat hepatocytes and HepG2 cells, the toxicity of CHR was the lowest among the five main components of rhubarb (Kang et al. 2017). It is noteworthy that CHR has an obvious neuroprotective effect in in vivo and in vitro experiments, and its mechanism is related to the inhibition of inflammatory reaction (Chae et al. 2017a, b), antioxidant (Lin et al. 2015), inhibition of Tau hyperphosphorylation (Ye et al. 2020a), and reduction of mitochondrial autophagy (Cui et al. 2022).

In our recent study, we discovered that CHR might improve learning and memory in AD model rats and had a neuroprotective effect on Aβ-induced PC12 cells, which could be connected to the inhibition of tau hyperphosphorylation and the CaM-CaMKIV signal pathway (Ye et al. 2020a, b, c). Our recent study found that CHR plays a neuroprotective role by interfering with the ERS-apoptosis pathway in the AD model (Li et al. 2022a, b). The experimental evidence supports that TXNIP is activated by ERS and contributes to the activation of the NLRP3 inflammatory cascade in the hippocampus of the AD brain (Ismael et al. 2021). Effective regulation of the ROS/TXNIP/NLRP3 signal pathway plays a positive role in the prevention and treatment of AD (Tsubaki et al. 2020). Based on the neuroprotective effect and ERS signal regulation of CHR, we hypothesized that CHR might prevent AD by regulating the ROS/TXNIP/NLRP3 signal pathway. Therefore, the study on the mechanism of CHR on AD targeting oxidative stress and inflammation can be the innovation point. In vivo and in vitro AD models were used to observe the regulatory effect of CHR on ROS/TXNIP/NLRP3 pathway, and to provide the experimental basis for its clinical application in AD.

Materials and methods

Reagents

CHR (purity = 98%, B20238) was purchased from Shanghai Yuanye Biotechnology Co., LTD., Verapamil hydrochloride (Ver) (purity = 99.98%, HY-A0064) were from MedChemExpress (MCE) (Fig. 1A). The dose of CHR used in vivo (0.35 mg/kg) and the concentration of CHR used in vitro (50 μM) based on previous studies (Ye et al. 2020a, b, c). D-galactose was purchased from Sinopharm Chemical Reagent Co., LTD. Aβ$_{25\text{-}35}$ (1 mg, A4559) was purchased from Sigma. Reactive oxygen species detection kit (CA1410) was obtained from Solarbio Science & Technology Co., Ltd. (Beijing, China). The concentrations of Aβ$_{25\text{-}35}$ in vivo (2 mg/mL) and in vitro (30 μM) were derived from the previous studies (Cai et al. 2018; Wang et al. 2016). MTT (ZP1104) was purchased from Hefei Zhenwo Biomedical Technology Co., Ltd (China). Hoechst33258 (BL804A), ECL chemiluminescence substrate kit (BL520B), reverse transcription kit (BL696A) were purchased from Biosharp (China). Lactate dehydrogenase (LDH, A020-2-2), Malondialdehyde (MDA, A003-1-2), Superoxide dismutase (T-SOD, A001-1-1), Catalase (CAT, A007-1-1), and Glutathione (GSH, A006-2-1) were purchased from Nanjing Jiancheng Bioengineering Insitute. Annexin V-FITC/PI kit (G1511), and SYBR (G3326-15) were purchased from Servicevbio Biotechnology Co., Ltd (Wuhan, China). Anti-TXNIP (DF7506), anti-Cleaved-caspase-1 (AF4005), anti-IL-1β (AF5103), and anti-IL-18 (DF6252) were purchased from Affinity Biosciences. Anti-TRX (ab273877) and anti-NLRP3 (Ab263899) were obtained from Abcam. Anti-GAPDH (KK1021) was purchased from ZEN-BIO SCIENCE
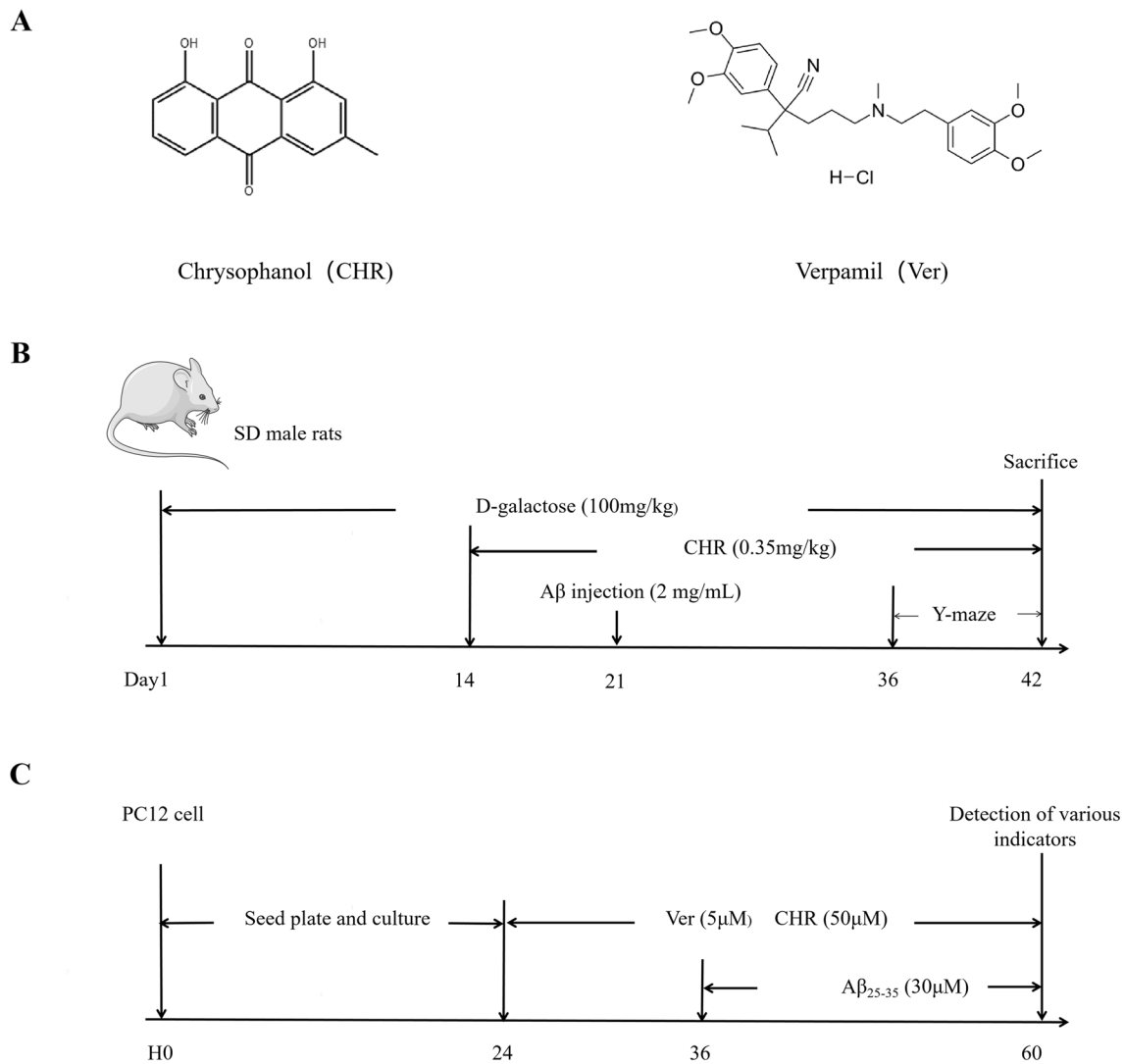
Fig. 1 Experimental design scheme. **A** chemical structure of CHR and Verpamil. **B** In vivo experiment. **C** In vitro experiment

(Chengdu, China). PC12 cells were obtained from the Shanghai Institute of Biochemistry and Cell Biology.

Animal modeling and drug administration

60 male Sprague–Dawley (SD) rats (10 months old, 250–300 g, SXCK (Lu) 20,190,003) were obtained from Jinan Pengyue Experimental Animal Breeding Co., Ltd. The Experimental Animal Ethics Committee at the Anhui University of Chinese Medicine authorized all experiments (Ethical certification number: 2022031, 7 November 2022). All rats were randomly divided into the Control group, Aβ$_{25\text{-}35}$ group (2 mg/mL Aβ$_{25\text{-}35}$) and Aβ$_{25\text{-}35}$+CHR group (2 mg/mL Aβ$_{25\text{-}35}$+0.35 mg/kg CHR), with 20 rats in each group. The AD rat model was established with

an intraperitoneal injection of D-galactose (100 mg/kg) and bilateral hippocampus injection of Aβ$_{25\text{-}35}$. In brief, Aβ$_{25\text{-}35}$ group and Aβ$_{25\text{-}35}$+CHR group were intraperitoneally injected with D-galactose once a day for 42 days. After 14 days of intraperitoneal injection of D-galactose, CHR was given by continuous gavage for 28 days, while the control group was given normal feeding. After 21 days of intraperitoneal injection of D-galactose, Aβ$_{25\text{-}35}$ group and Aβ$_{25\text{-}35}$+CHR group were anesthetized by pentobarbital sodium (40 mg/kg) and fixed on a brain stereotactic instrument. Brain stereoscopic locator selected the anterior fontanelle as the starting point, the puncture point 4.4 mm back, 2.2 mm lateral, needle distance from the brain surface 3.0 mm. 5 μL (10 μg) of Aβ$_{25\text{-}35}$ was injected into the

bilateral hippocampus with a microsyringe pump (Fig. 1B) (Ye et al. 2020a, b, c).

Y-maze test

Y-maze test was performed on the 36th day after D-galactose injection to evaluate the learning, memory and exploration ability of the rats. Each rat was placed into the maze from the central area of the triangle and allowed to move freely in the maze for 10 min without interference. The activity tracking of the rat was recorded by the camera. The rats first moved in the space of the occluded third arm, and then opened the occluded third arm to detect the movement trajectory of the rats for 5 min. Rats entering different arms from the previous two times were regarded as correct arm entry. The proportion of times the rats entered the new arm and the distance in the new arm were counted (Sun et al. 2021).

Hematoxylin–eosin (H&E) staining

The brain tissue was fixed with 4% paraformaldehyde, dehydrated, embedded in paraffin, and sliced at 5 μm. Morphological changes of hippocampal CA1, CA3 and DG neurons were observed with BX51 positive microscope (Xuan et al. 2020).

AD cell model establishment, cell viability analysis and drug administration

AD cell model was established by 30 μM $A\beta_{25-35}$ intervention on PC12 cells. The optimal concentration of CHR was investigated by 3-(4,5-dimethylthiazol-2-yl)-2, 5-diphenyltetrazolium bromide (MTT) assay. PC12 cells were inoculated into 96-well plate with 5×10^4/mL. After incubation for 24 h, the cells were pretreated with 12.5, 25, 50 and 100 μM of CHR for 12 h, and then $A\beta_{25-35}$ was added for 24 h. PC12 cells were divided into the Control group, $A\beta_{25-35}$ group (30 μM $A\beta_{25-35}$), $A\beta_{25-35}$+CHR group (30 μM $A\beta_{25-35}$+50 μM CHR), $A\beta_{25-35}$+Ver group (30 μM $A\beta_{25-35}$+5 μM Ver) and $A\beta_{25-35}$+CHR+Ver group (30 μM $A\beta_{25-35}$+50 μM CHR+5 μM Ver). After incubation for 24 h, cells were stimulated with 50 μM CHR and 5 μM Ver for 12 h before modeling, and continued to culture for 24 h after modeling for subsequent experiments (Fig. 1C).

Reactive oxygen species (ROS) detection

DCFH-DA fluorescence probe was used to evaluate the intracellular ROS level. Adjust cell density to 1×10^5 cells/mL, inoculated into a 6-well plate, and then mixed with 10 μM DCFH-DA was cultured in serum-free medium for 20 min. After PBS was washed, fluorescence intensity was observed with fluorescence microscope (Leica, Germany) (Liu et al. 2022a, b, c).

Cell apoptosis detection

The cell apoptosis was detected by Hoechst and Annex-inV/PI double staining. Cell density adjusted to 1×10^5 cells/mL were inoculated in a 12-well plate. The treated cells were fixed with 4% paraformaldehyde for 30 min, then incubated with Hoechst33258 in the dark for 5 min, and observed under a fluorescence microscope (Leica, Germany). Annexin V-FITC and PI were added according to the instructions of the kit. The apoptosis rate was detected by flow cytometry (FACS Celesta, BD, USA), and the data were analyzed by FlowJo 7.6 (Chen et al. 2020; Liu et al. 2015).

Oxidative stress index detection

The content of LDH in rat hippocampal tissue and PC12 cell culture supernatant, and the contents of MDA, T-SOD, CAT, and GSH in rat hippocampal tissue and PC12 cells were detected by colorimetric method. The absorbance values were measured at 450 nm, 532 nm, 550 nm, and 405 nm by a microplate reader (Multiskan Spectrum, USA) according to corresponding kit instructions (Li et al. 2022a, b).

Protein expression detection

Rat hippocampal tissue and PC12 cells were lysed in RIPA buffer. The lysate was centrifuged at 12,000 rpm at 4 °C for 15 min, and the total protein was extracted by precipitation. After protein quantification with the BCA analysis kit, 10–15% SDS-PAGE was used to separate the equal amounts of total protein and transferred to the PDVF membrane. After blocking with 5% skim milk powder for 2 h and washing 3 times × 10 min, primary antibodies TXNIP (1:1000), TRX (1:500), NLRP3 (1:1000), Cleaved caspase-1 (1:1000), IL-1β (1:1000), IL-18 (1:1000) and GAPDH (1:5000) were added and incubated overnight at 4 °C. The secondary antibody was incubated again for 1.5 h after washing the membrane 3 times × 10 min. Enhanced chemiluminescence (ECL) kit was used for visualization, and the image was presented on the Tanon 5200 chemiluminescence imaging system (Tanon, Shanghai), and the gray value of the bands were analyzed by image J (Li et al. 2020a, b).

mRNA expression detection

The mRNA expressions of target genes were detected by RT-PCR. After the rat hippocampus and treated PC12 cells were collected, total RNA was extracted with Trizol reagent, and RNA was quantified. RNA purity was determined based on its absorbance on a UV spectrophotometer at 260 and 280 nm. The RNA was reverse transcribed into cDNA using a reverse transcriptometer (Mastercycler® nexus gradient, Germany) and then analyzed using a LightCycler 96 real-time PCR instrument (Roche, Switzerland). The reaction conditions were set as follows: (1) 95 °C for 15 s, (2) 60 °C for 60 s, (3) 72 °C for 30 s. After 40 cycles of amplification, the mRNA expression levels of the genes were analyzed by $2^{-\Delta\Delta Cq}$ method with β-actin as control (Lian et al. 2018). Primer sequences were shown in Table 1.

Molecular docking

CB-DOCK platform was utilized to predict the binding affinity of CHR or Ver to TXNIP. TXNIP (PDB ID: 4GEI) (Polekhina et al. 2013) and CHR or Ver SDF formats were input to CB-Dock (Liu et al. 2022a, b, c).

Statistical analysis

SPSS 26.0 software was used for data analysis, expressed as mean ± standard deviation (SD). One-way analysis of variance was used to compare the mean values among multiple groups, and $P < 0.05$ had significant differences.

Table 1 Primers used in RT-PCR

Primers		Sequence (5′→3′)
TXNIP	Forward	5′-CCAGACCAAAGTGCTCACTCAGAAG-3′
	Reverse	5′-GAGACTCTTGCCACGCCATGATG-3′
TRX	Forward	5′-AAGCCCTTCTTTCATTCCCTCTGTG-3′
	Reverse	5′-CAGCAACATCCTGGCAGTCATCC-3′
NLRP3	Forward	5′-GAGCTGGACCTCAGTGACAATGC-3′
	Reverse	5′-AGAACCAATGCGAGATCCTGACAAC-3′
Caspase-1	Forward	5′-GCACAAGACTTCTGACAGTACCTTCC-3′
	Reverse	5′-GCTTGGGCACTTCAATGTGTTCATC-3′
IL-1β	Forward	5′-AATCTCACAGCAGCATCTCGACAAG-3′
	Reverse	5′-TCCACGGGCAAGACATAGGTAGC-3′
IL-18	Forward	5′-CGACCGAACAGCCAACGAATCC-3′
	Reverse	5′-GTCACAGCCAGTCCTCTTACTTCAC-3′
β-actin	Forward	5′-CCCATCTATGAGGGTTACGC-3′
	Reverse	5′-TTTAATGTCACGCACGATTTC-3′

Results

In vivo results

CHR meliorated cognitive deficits in AD rats

Compared with the control group, percentage of times of rats entering the novel arm, and the percentage of a distance of rats in the novel arm in the Aβ$_{25-35}$ group were reduced ($P < 0.01$). CHR significantly improved the activity of rats in the novel arm (Fig. 2). CHR could improve learning and memory.

CHR ameliorated hippocampal neuron damage and oxidative stress in AD rats

Aβ$_{25-35}$ induced hippocampal neuronal damage is related to learning and cognitive impairment in AD rats (Ge et al. 2021). In the control group, the hippocampal neuron cells were intact and arranged neatly, while the neurons in the Aβ$_{25-35}$ group were changed, mainly includes sparse neurons, disordered arrangement, morphological shrinkage, deep staining, cell body deformation and obvious rupture. Compared with Aβ$_{25-35}$ group, CHR treatment showed relatively uniform cell distribution and significantly recovered the neuronal damage caused by Aβ$_{25-35}$ (Fig. 3A). ROS is the key factor in the occurrence of oxidative stress, and the excessive accumulation can produce the lipid peroxidation product MDA and release LDH (Li et al. 2020a, b). T-SOD, CAT and GSH are important antioxidants, and the activities are used to evaluate the scavenging ability of ROS. Compared with the control group, the levels of MDA and LDH in the serum of rats in Aβ$_{25-35}$ group increased significantly, while the activities of T-SOD, CAT and GSH decreased significantly ($P < 0.01$) (Fig. 3B–F). CHR intervention significantly reversed the expression of oxidative stress index ($P < 0.01$, $P < 0.05$). CHR alleviated the changes of hippocampal neurons and oxidative stress injury induced by AD rats.

CHR inhibited the activation of TXNIP and NLRP3 in AD rats

Oxidative stress causes inflammation, and TXNIP activation can further trigger NLRP3 inflammasome activation (Yang et al. 2022). The effects of CHR on TXNIP and NLRP3 in AD rats were analyzed. Compared with the control group, the protein expressions of TXNIP, NLRP3, Cleaved caspase-1, IL-1β and IL-18 in Aβ$_{25-35}$ group were significantly increased, and TRX was significantly decreased ($P < 0.01$) (Fig. 4A,B). The results of RT-PCR were consistent with the trend of protein expression ($P < 0.01$) (Fig. 4C). CHR administration significantly reversed oxidative stress and

Fig. 2 Effects of CHR on learning and memory in AD rats. **A** Heat map of Y-maze experiment. **B** Percentage of times of rats in each group entering the novel arm. **C** Percentage of a distance of rats in each group in the novel arm. Data are expressed as mean ± SD, $n = 8$. **$P < 0.01$, vs. Control group; ##$P < 0.01$, vs. Aβ_{25-35} group
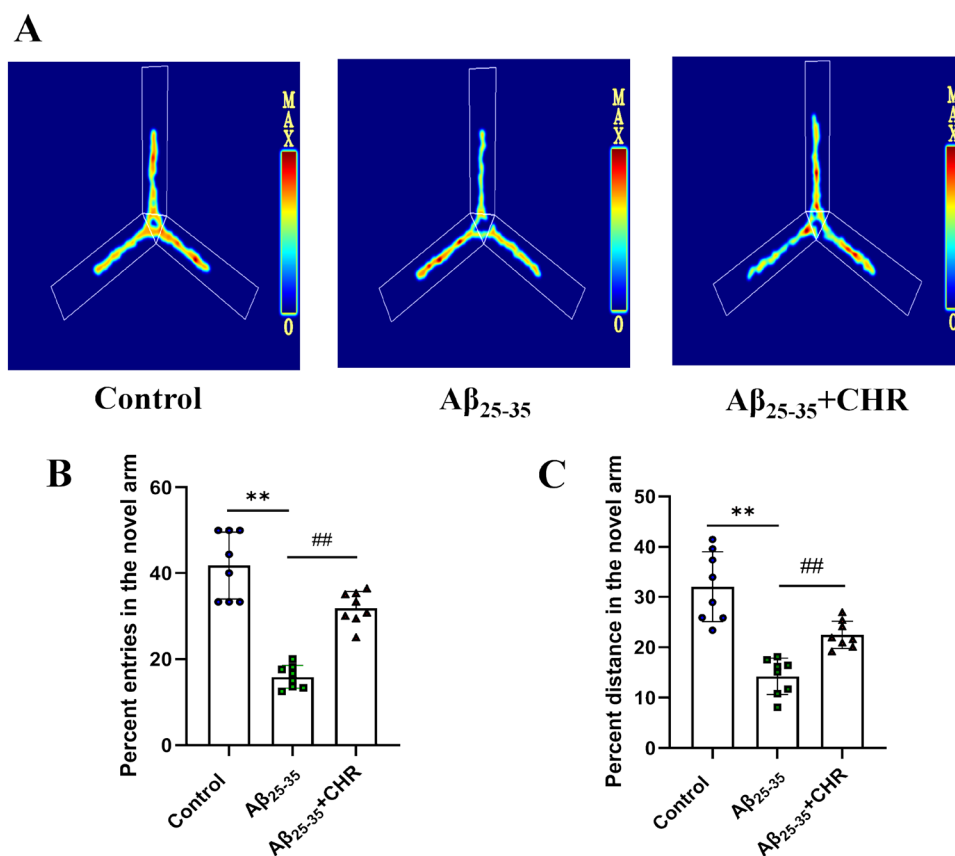
inflammatory damage caused by Aβ_{25-35} ($P < 0.01$, $P < 0.05$) (Fig. 4A–C). The protection of CHR on AD was related to the inhibition of TXNIP and NLRP3 activation. Next, the mechanism of CHR was further studied in vitro.

In vitro results

Protective effect of CHR on AD cell

The protective effect of different concentrations of CHR on AD cell injury was investigated, and then the optimal concentration was optimized. Compared with the control group, the cell viability of Aβ_{25-35} group was significantly decreased ($P < 0.01$). Compared with Aβ_{25-35} group, 12.5, 25 and 50 μM of CHR significantly improved cell survival ($P < 0.01$), the survival rate decreased at 100 μM, hence, 50 μM of CHR showed the best protective effect, as previously reported(Fig. 5A).

CHR inhibited oxidative stress and apoptosis induced by Aβ_{25-35} in PC12 cells

ROS fluorescence intensity was significantly increased, the levels of MDA and LDH were increased, and the activities of T-SOD, CAT and GSH were decreased in Aβ_{25-35} group

($P < 0.01$). CHR could inhibit ROS production, decrease the levels of MDA and LDH, and increase the activities of T-SOD, CAT and GSH ($P < 0.01$) (Fig. 5B–D). Apoptosis is a cell death process that plays an important role in neurodegeneration and is influenced by ROS (Yang et al. 2021). After the accumulation of intracellular ROS, the scavenging ability of ROS will be decreased, and when the antioxidant ability is weakened, apoptosis will be caused (Kang et al. 2019). Compared with the control group, the apoptosis rate of the Aβ_{25-35} group was significantly increased ($P < 0.01$). CHR administration significantly reduced cell apoptosis and promoted cell growth ($P < 0.01$) (Fig. 5E,F). CHR could inhibit oxidative stress damage and apoptosis.

CHR inhibited TXNIP and NLRP3 activation in PC12 cells induced by Aβ_{25-35}

Compared with the control group, the protein expressions of TXNIP and NLRP3 in Aβ_{25-35} group were significantly up-regulated, the mRNA levels of TXNIP, NLRP3, Caspase-1, IL-1β and IL-18 were significantly increased, and the mRNA level of TRX was significantly decreased ($P < 0.01$). CHR treatment significantly reversed protein and mRNA expressions (Fig. 6).
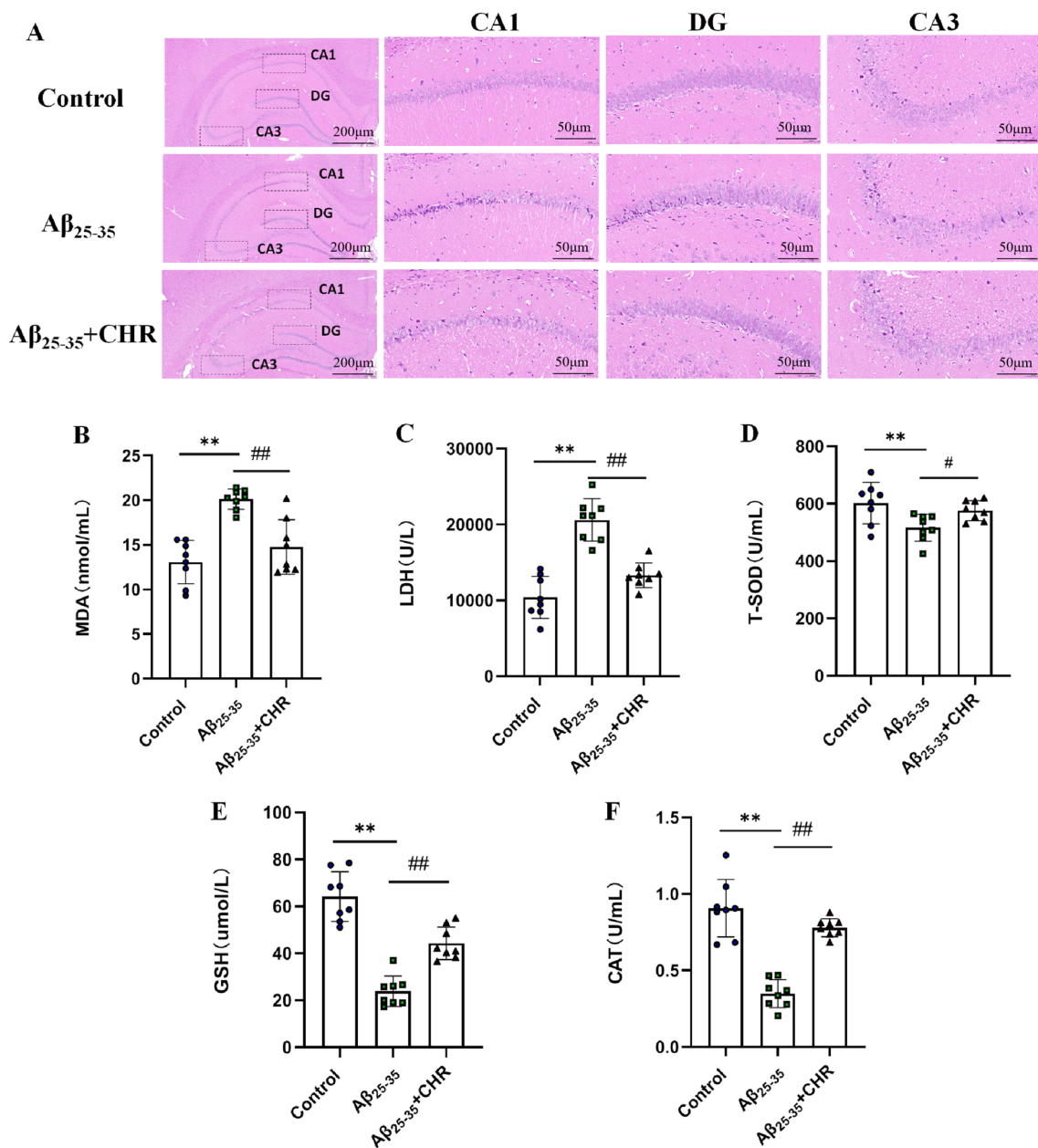
Fig. 3 Effects of CHR on rat hippocampal neuron injury and oxidative stress. **A** H&E staining. Scale bar for the overall picture of the hippocampus (200 μm). Scale bar for the picture of CA1, DG, and CA3 regions (50 μm). **B** MDA. **C** LDH. **D** T-SOD. **E** CAT. **F** GSH. $n = 8$. **$P < 0.01$, vs. Control group; #$P < 0.05$, ##$P < 0.01$, vs. Aβ$_{25\text{-}35}$ group

CHR reduced ROS production and apoptosis in PC12 cells by inhibiting TXNIP

Compared with the control group, the fluorescence intensity of ROS in Aβ$_{25\text{-}35}$ group was significantly increased. Hoechst staining showed that the nuclei of Aβ$_{25\text{-}35}$ group showed a large amount of bright blue, showing typical characteristics of apoptosis. Flow cytometry showed that the apoptosis rate increased significantly. Compared with the Aβ$_{25\text{-}35}$ group, the ROS fluorescence intensity in the Aβ$_{25\text{-}35}$ + CHR group,
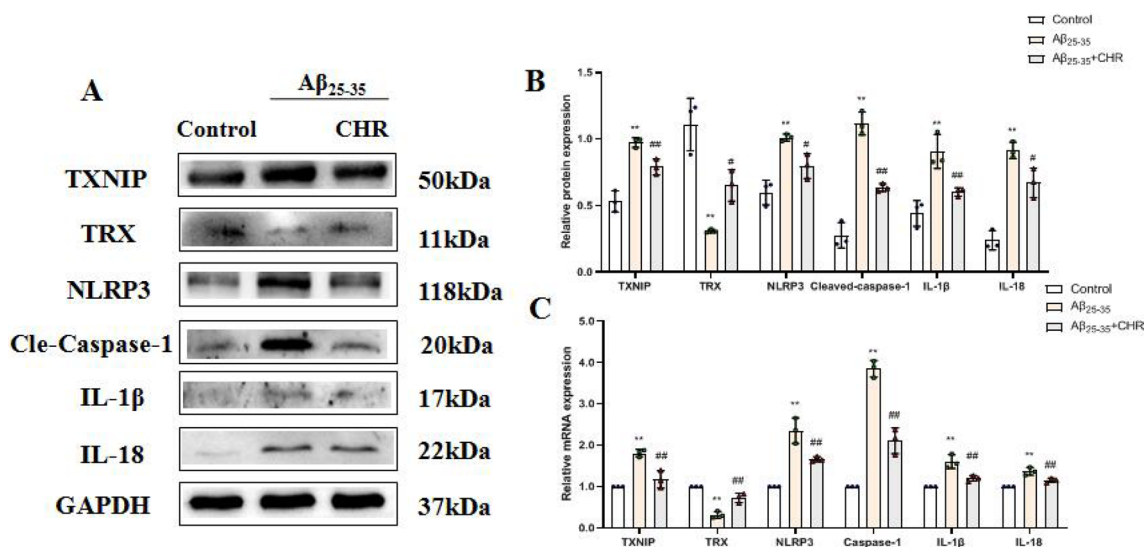
Fig. 4 Effect of CHR on the activation of TXNIP and NLRP3 in the hippocampus of AD rats. **A** Representative immunoblots for TXNIP, TRX, NLRP3, Cleaved-caspase-1, IL-1β, and IL-18. **B** The protein expressions of TXNIP, TRX, NLRP3, Caspase-1, IL-1β, and IL-18 proteins. **C** Relative mRNA levels of TXNIP, TRX, NLRP3, caspase-1, IL-1β and IL-18. $n = 3$. **$P < 0.01$, vs. Control group; #$P < 0.05$, ##$P < 0.01$, vs. Aβ$_{25\text{-}35}$ group

the Aβ$_{25\text{-}35}$ + Ver group, and the Aβ$_{25\text{-}35}$ + CHR + Ver group was significantly weakened, the nuclear staining was significantly lighter, and the apoptosis rate was greatly reduced, especially in the Aβ$_{25\text{-}35}$ + CHR + Ver group ($P < 0.01$) (Fig. 7). CHR may protect the development of AD induced by Aβ$_{25\text{-}35}$ by inhibiting TXNIP.

CHR protected against Aβ$_{25\text{-}35}$-induced injury by regulating ROS/TXNIP/NLRP3 pathway

To further support this hypothesis, compared with the Aβ$_{25\text{-}35}$ group, the protein expressions of TXNIP, NLRP3, Cleaved caspase-1, IL-1β and IL-18 in Aβ$_{25\text{-}35}$ + CHR group, Aβ$_{25\text{-}35}$ + Ver group and Aβ$_{25\text{-}35}$ + CHR + Ver group were significantly decreased, while the protein expression of TRX was increased, especially in Aβ$_{25\text{-}35}$ + CHR + Ver group ($P < 0.01$, $P < 0.05$) (Fig. 8A–F). In addition, the expression results of PCR in each group were consistent with the protein expression results ($P < 0.01$, $P < 0.05$) (Fig. 9A–F). Ver directly reduces the expression of TXNIP and further protects PC12 cells when CHR is combined with verapamil. All these results indicated the neuroprotective effect of CHR on the inhibition of TXNIP generation and reduction of oxidative stress and inflammatory damage.

Docking results

On the basis of the in vivo and in vitro experimental results, we conducted molecular docking to verify the experimental results, and the results were found to be consistent with the experimental results. The interaction between CHR or Ver and TXNIP was investigated by molecular docking. The results showed that, compared with the positive control drug, under the condition of the same cavity size and the central coordinates of the docking pocket, the docking vina score of CHR and TXNIP was—6.6, and its docking score was equivalent to Ver, or even lower. Notably, the binding sites of amino acid residues between CHR and TXNIP were similar to those of Ver. Therefore, CHR had a good binding affinity with TXNIP, and its binding activity was comparable to Ver (Table 2, Fig. 10).

Discussion

The primary pathology features of AD include senile plaques (SP) created by amyloid β-protein (Aβ) deposition, neurofibrillary tangles (NFTs) formed by abnormal Tau phosphorylation and aggregation, and significant hippocampus cell loss (Ashrafian et al. 2021). The abnormal deposition of Aβ protein, hyperphosphorylation of Tau, oxidative stress, inflammatory response, autophagy, ApoE hypothesis, excitatory nerve injury theory, and cholinergic hypothesis are the molecular mechanisms used to treat AD (Khan et al. 2020; Srivastava et al. 2021). More and more evidence showed that oxidative stress and inflammatory responses in brain tissue play a substantial role in AD (Nasoohi et al. 2018). Hence, regulate oxidative stress, decrease ROS generation, and then prevent cell apoptosis
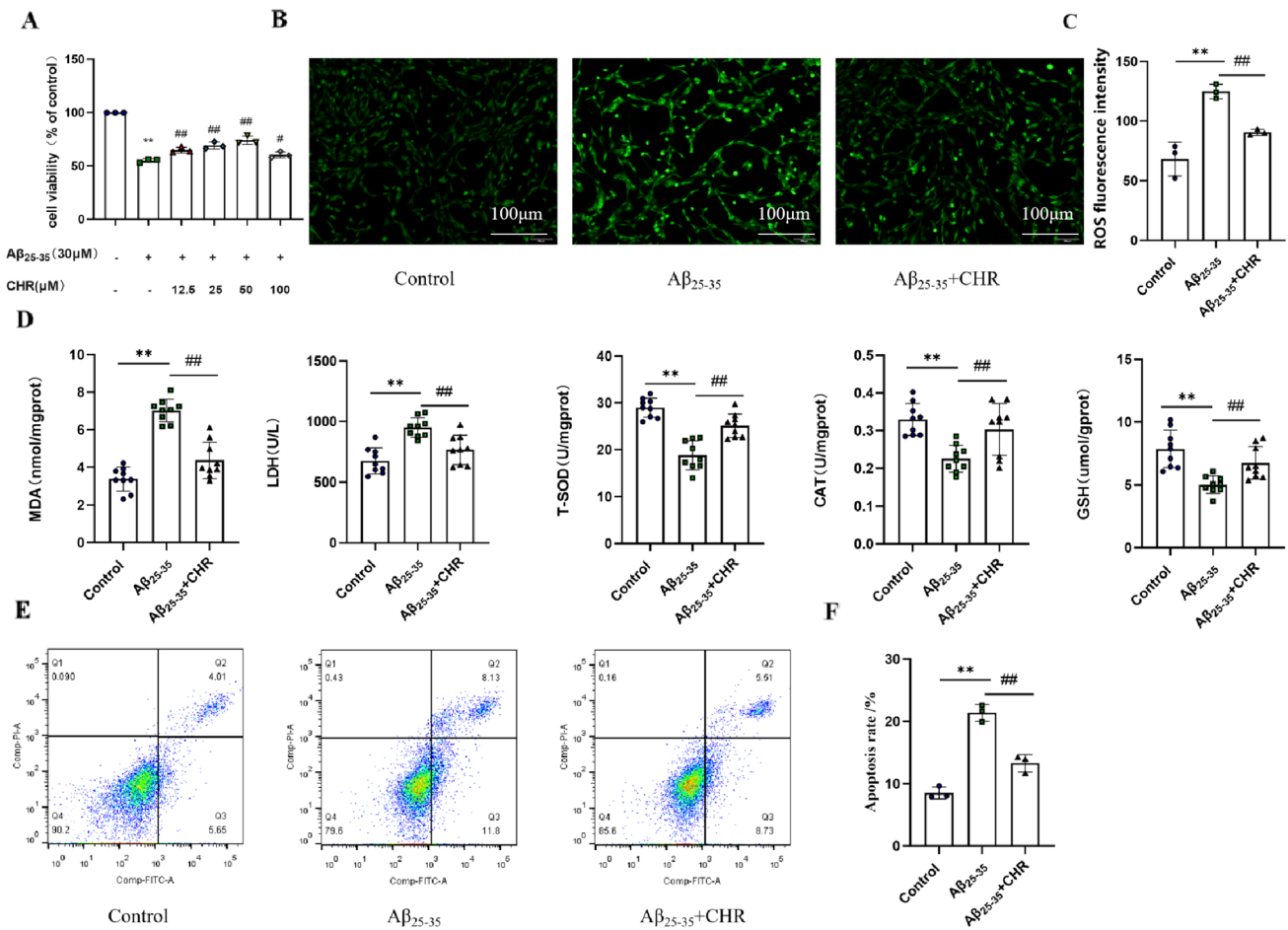
Fig. 5 Effects of CHR on oxidative stress and apoptosis in Aβ$_{25-35}$-induced PC12 cells. **A** Effects of CHR (12.5, 25, 50 and 100 μM) on survival rate. **B** Representative image of ROS fluorescence intensity. Scale bar for the picture (100 μm). **C** ROS fluorescence intensity. **D** MDA, LDH, T-SOD, CAT and GSH levels. **E** PC12 cells apoptosis. **F** Apoptosis rate. Data are expressed as mean ± SD. **$P < 0.01$, vs. Control group; #$P < 0.05$, ##$P < 0.01$, vs. Aβ$_{25-35}$ group

and downstream inflammation to have a neuroprotective function in AD.

As a neurotoxin, Aβ has been widely used to establish AD models in vivo and in vitro. Previous studies have shown that Aβ$_{25-35}$ aggregates located around neurons are directly toxic to neurons, thereby inducing neuronal apoptosis. Intraperitoneal injection of D-galactose can destroy the balance between osmotic pressure and cell morphology, thereby accelerating aging and cognitive dysfunction (Gao et al. 2015; Wei et al. 2017). Therefore, this study used the combination of D-GALACTOSE and Aβ$_{25-35}$ to establish the AD rat model. In addition, previous studies found that PC12 cells treated with 30 μM Aβ$_{25-35}$ for 24 h were determined by MTT assay to induce the establishment of AD cell model, which provided a good basis for the follow-up experiment (Cai et al. 2018).

TXNIP is an important regulator involved in the process of oxidative stress. TXNIP has an α-inhibitor domain that drives the transport of cellular proteins. Under normal conditions, TXNIP localizes in the nucleus, but it can translocate

in response to different stimuli. TXNIP may be transferred to mitochondria and block the ROS scavenging activity of TRX2, thus leading to oxidative stress. TXNIP also controls the nuclear translocation of NF-κB, thereby inducing inflammatory damage (Domingues et al. 2021). In the cytoplasm, TXNIP is associated with NLRP3 inflammasome activation. As an endogenous inhibitor of the antioxidant and apoptotic protein TRX, TXNIP can bind to the active site of TRX, thereby inhibiting the activity of TRX and promoting the production and aggregation of ROS. With the accumulation of ROS, the oxidation–reduction equilibrium system in the cell is disturbed, and the oxidative stress program is initiated, which induces TXNIP translocation from the nucleus to the cytoplasm, activates NLRP3 inflammasome, then activates Caspase-1 and releases inflammatory factors IL-1β and IL-18 (Fig. 11), which eventually causes neuroinflammatory injury and apoptosis. Inhibition or knockdown of TXNIP has a significant neuroprotective effect (Han et al. 2018). Down-regulation of TXNIP expression inhibited
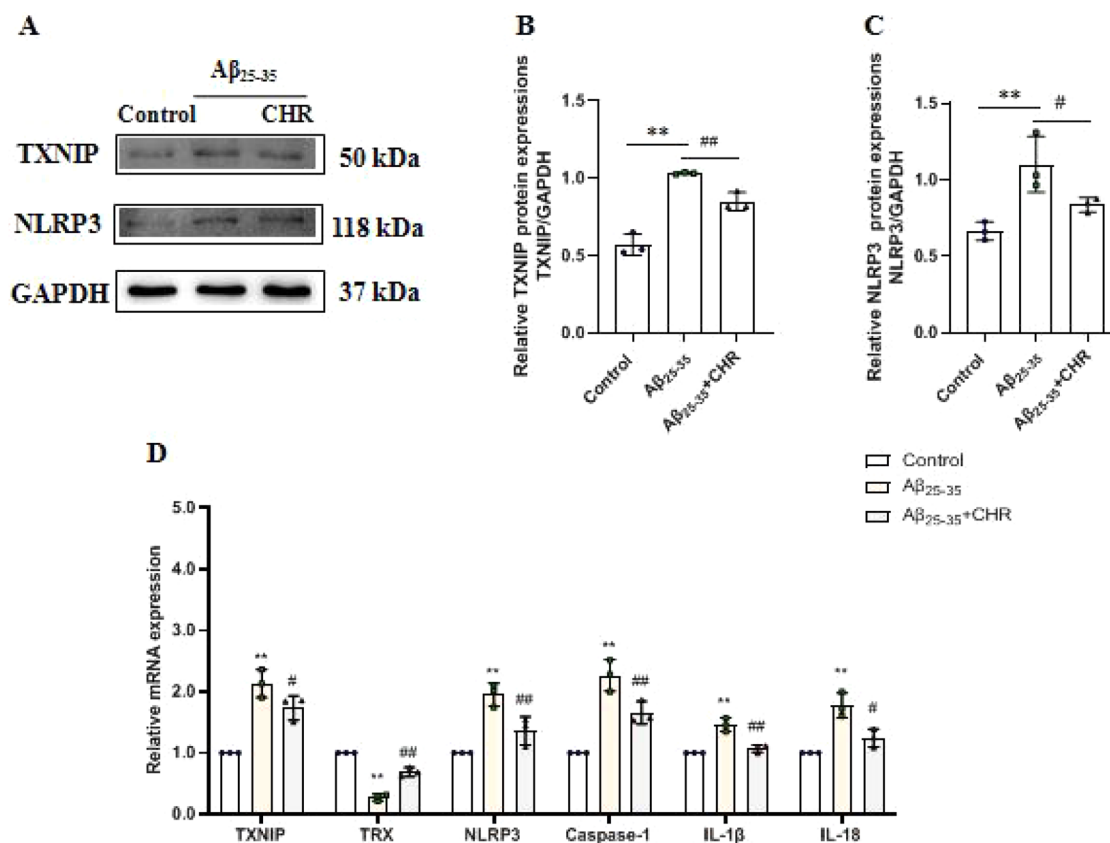
Fig. 6 Effect of CHR on TXNIP and NLRP3 activation induced by Aβ$_{25-35}$ in PC12 cells. **A** Representative immunoblots for TXNIP and NLRP3. **B** The protein expressions of TXNIP. **C** The protein expressions of NLRP3. **D** Relative mRNA levels of TXNIP, TRX, NLRP3, Caspase-1, IL-1β and IL-18. Data are expressed as mean ± SD. **$P < 0.01$, vs. Control group; #$P < 0.05$, ##$P < 0.01$, vs. Aβ$_{25-35}$ group

corticosterone-induced inflammatory activation in microglia, which in turn activated Caspase-1 activity and released the inflammatory factor IL-1β (Bharti et al. 2019). Rutin could significantly decrease ROS production and inhibit the expression of TXNIP, NLRP3, caspase-1 and IL-1β to protect the endothelial dysfunction (Wang et al. 2017). Therefore, the natural products targeting TXNIP can effectively be used as a promising therapeutic modality for AD. Verapamil, a calcium channel blocker, is commonly used to treat cardiovascular disease. In recent years, it has also become an option for treating neurological diseases, including AD (Popović et al. 2020). Notably, verapamil, as an inhibitor of TXNIP, significantly reduced the 7-keto-induced increase in caspase-1 activity (Koka et al. 2017). Verapamil also reversed the upregulation of TXNIP activity resulting from ceramide treatment and reduced apoptosis (Shi et al. 2021). Verapamil can improve oxidative stress and inhibit Tau phosphorylation by inhibiting TXNIP, which plays a protective role in AD (Melone et al. 2018). In addition, verapamil inhibited TXNIP-NLRP3 inflammasome activation and improved cognitive function after intracerebral hemorrhage (ICH) in mice (Ismael et al. 2022). Therefore, verapamil

can be used as a good TXNIP inhibitor to participate in the treatment of AD in this study.

Studies have shown that CHR, as an anthraquinone compound, has better absorption capacity and digestion speed in its family (Yusuf et al. 2019). Chen et al. found that CHR has a high plasma protein binding rate, and its content in the kidney is higher than that in the liver, indicating that it is eliminated through excretion rather than metabolism. In addition, CHR has good intestinal absorption and cannot easily penetrate the blood–brain barrier (Chen et al. 2014; Sreelakshmi et al. 2017), but it can improve the nerve injury, brain edema and blood–brain barrier rupture of I/R in a dose-dependent manner (Zhang et al. 2014). Because CHR is not easily soluble in water, it is often prepared into suspension, which can be administered repeatedly by gavage under the condition of ensuring the uniformity and stability of the drug, and is safe and reliable. Based on our previous studies and verification, we found that 0.35 mg/kg dose and 50 μM concentration had the best protective effect on Aβ$_{25-35}$-induced AD rats and PC12 cell models. In addition, CHR plays an important role in the treatment of ischemic stroke, cerebral hemorrhage, traumatic brain injury, brain tumor, AD and other central

A

Control Aβ$_{25-35}$ Aβ$_{25-35}$+CHR Aβ$_{25-35}$+Ver Aβ$_{25-35}$+CHR+Ver

B

C

Control Aβ$_{25-35}$ Aβ$_{25-35}$+CHR

Aβ$_{25-35}$+Ver Aβ$_{25-35}$+CHR+Ver

D

Control Aβ$_{25-35}$ Aβ$_{25-35}$+CHR
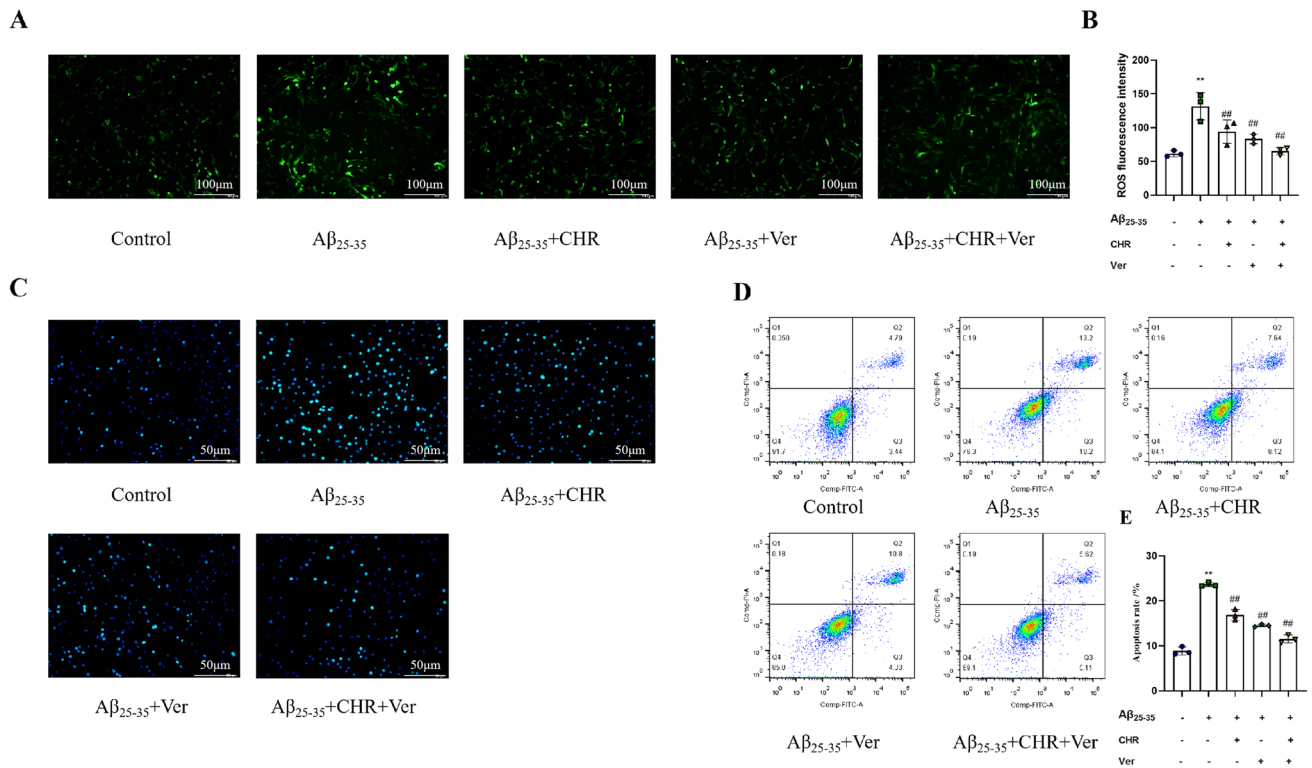
E

Aβ$_{25-35}$+Ver Aβ$_{25-35}$+CHR+Ver

Fig. 7 CHR reduced ROS production and apoptosis in PC12 cells by inhibiting TXNIP. **A** Representative image of ROS fluorescence intensity. Scale bar for the picture (100 μm). **B** ROS fluorescence intensity. **C** Hoechst33258. Scale bar for the picture (50 μm). **D** Flow cytometry. **E** Apoptosis rate. Data are expressed as mean ± SD. **$P < 0.01$, vs. Control group; ##$P < 0.01$, vs. Aβ$_{25-35}$ group

nervous system diseases (Li et al. 2019). CHR could reduce the apoptosis induced by glutamate by inhibiting the pro-apoptotic factors of hippocampal neuronal cells, regulate the dephosphorylation of hippocampal Drp 1, reduce ROS level, inhibit mitochondrial fission, and play an antioxidant role (Chae et al. 2017a, b). CHR attenuates the pyroptosis of NLRP3 induced by cerebral ischemia–reperfusion injury in a TRAF6-dependent manner (Xia et al. 2022). In addition, CHR can protect the neuroinflammatory response after stroke by regulating the IL-6-STAT3 signal pathway (Liu et al. 2022a, b, c). Zhao et al. proved that CHR can inhibit heme-induced HT22 cell apoptosis, oxidative stress and endoplasmic reticulum stress response by regulating miR-320-5p/Wnt3a/β-Catenin signaling pathway, which can be used as an effective drug for treating cerebral hemorrhage (Zhao et al. 2022). Although the above studies indicate that CHR can be used as a potential therapeutic approach, the underlying mechanism of its treatment of AD still needs to be further investigated.

In this study, in vivo and in vitro experiments were conducted to investigate whether CHR could play a neuroprotective role in Aβ$_{25-35}$-induced AD model by regulating ROS/TXNIP/NLRP3 signaling pathway. Based on the previous experimental research, the combination of oxidative stress and inflammatory reaction for the first time has proved that CHR

can further inhibit the occurrence of downstream inflammation by inhibiting oxidative stress and reducing the accumulation of reactive oxygen species. In this process, TXNIP plays a key role as a bridge. Therefore, the ROS/TXNIP/NLRP3 signal pathway is important and innovative in studying the neuroprotective effect of CHR on AD. In animal models of AD, the Y-maze test, Morris water maze test and passive avoidance test are commonly used to detect learning, memory and spatial exploration ability (Shen et al. 2020). Y-maze test was used to evaluate the memory ability of rats in this study. After Aβ$_{25-35}$ injection, the rats showed significant cognitive impairment, the percentage of times rats entering the novel arm and the percentage of distance in the novel arm decreased, which indicates that the AD rat model was successfully established. CHR administration significantly reversed the above results, suggesting a significant improvement in neurological function. Aβ is the cleavage product of β-amyloid precursor protein, whose abnormal aggregation can lead to the death of hippocampal neurons (Zhao et al. 2020). CHR significantly ameliorated the neuronal damage induced by Aβ in rats. Excessive accumulation of ROS leads to oxidative stress injury and the release of cell damage marker LDH (Martínez et al. 2020). SOD, GSH and CAT are important antioxidant defense systems, and MDA is the final product formed by lipid peroxidation (Xu et al. 2018). In this study, after Aβ$_{25-35}$ stimulation of rats and
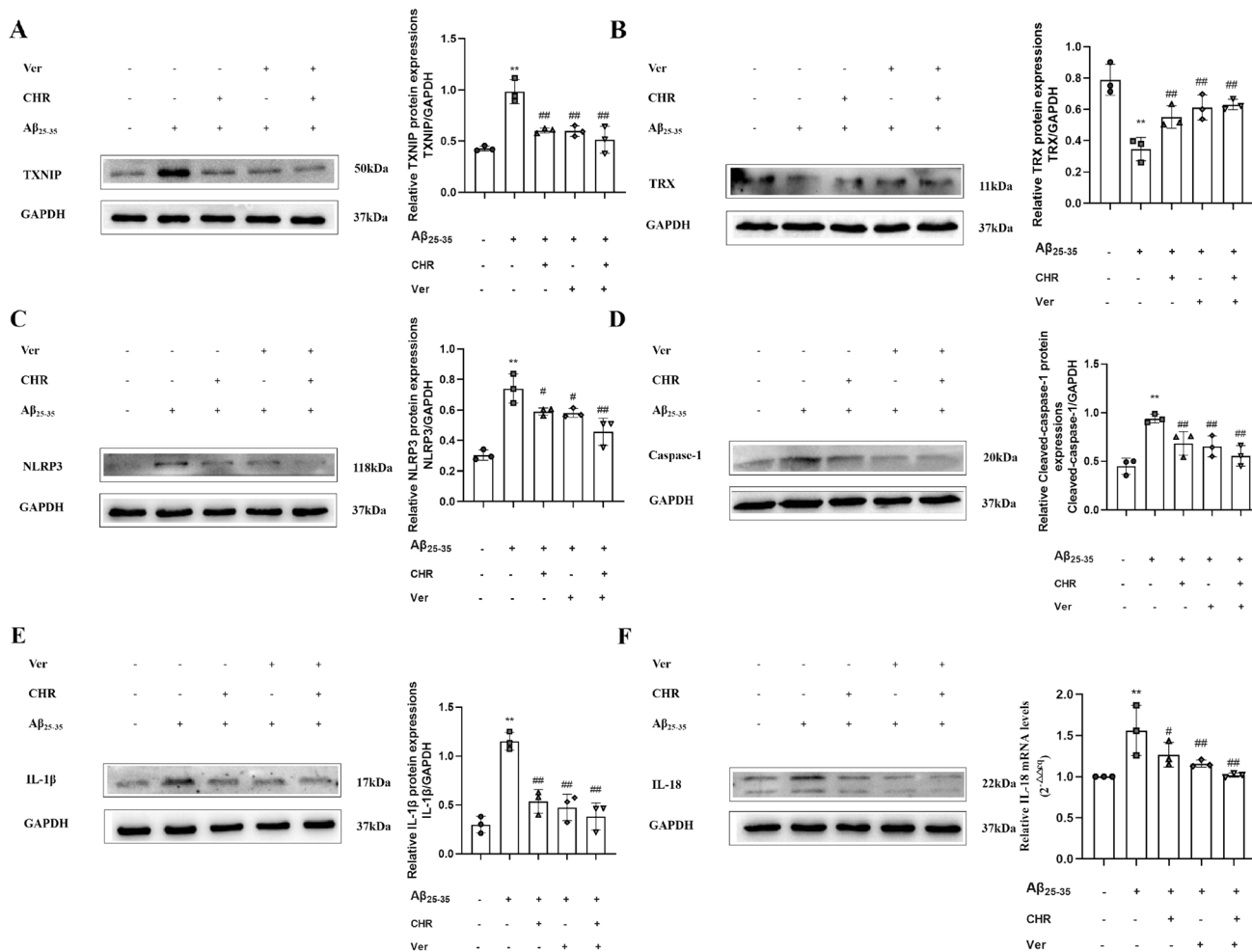
Fig. 8 Effect of CHR on the protein expressions of TXNIP, TRX, NLRP3, Cleaved-caspase-1, IL-1β and IL-18 in the AD cells. **A** TXNIP protein. **B** TRX protein. **C** NLRP3 protein. **D** Cle-caspase-1 protein. **E** IL-1β protein. **F** IL-18 protein. Data are expressed as mean ± SD. **$P < 0.01$, vs. Control group; #$P < 0.05$, ##$P < 0.01$, vs. Aβ$_{25-35}$ group

PC12 cells, the levels of LDH and MDA were significantly up-regulated, and the activities of T-SOD, CAT and GSH were significantly decreased. CHR and Ver intervention reversed the damage caused by Aβ$_{25-35}$. These results indicate that CHR has a potential antioxidant effect in Aβ$_{25-35}$-induced AD models. ROS can act as an inflammatory signal and play a key role in the activation of NLRP3 (Minutoli et al. 2016). As a key junction point between oxidative stress and neuroinflammation, TXNIP dissociates from TRX under oxidative stress and binds to downstream NLRP3 to trigger inflammation and apoptosis (Wang et al. 2020). The protective effect of CHR on Aβ$_{25-35}$-induced apoptosis of PC12 cells was confirmed by Hoechst and flow cytometry. In this study, after Aβ$_{25-35}$ induced brain injury, the protein expression and mRNA levels of TXNIP, NLRP3, Caspase-1, IL-1β and IL-18 were significantly increased, while the expression of TRX was significantly decreased. CHR could significantly reverse the expression of these targets, indicating that CHR reduced oxidative stress and

inflammatory damage in vitro and in vivo. To further illustrate the neuroprotective mechanism of CHR in AD model by regulating ROS/TXNIP/TXNIP signaling pathway, inhibition of TXNIP with verapamil in vitro can inhibit oxidative stress and inflammation, and reduce ROS generation. After inhibition of TXNIP with verapamil, the ROS fluorescence intensity and apoptosis rate were significantly decreased, and the protein expression and mRNA levels of TXNIP, NLRP3, Caspase-1, IL-1β and IL-18 were significantly decreased, and the protein expression and mRNA level of TRX were significantly increased. CHR and Ver played the same role, and the combination of CHR and Ver had a particularly significant effect. In short, Aβ$_{25-35}$ stimulates the occurrence of oxidative stress, which leads to apoptosis and downstream neuroinflammatory response, in which TXNIP acts as a key target of oxidative stress. CHR has a neuroprotective effect on AD by inhibiting TXNIP, thus blocking oxidative stress, inhibiting TXNIP and TRX separation, reducing apoptosis, and
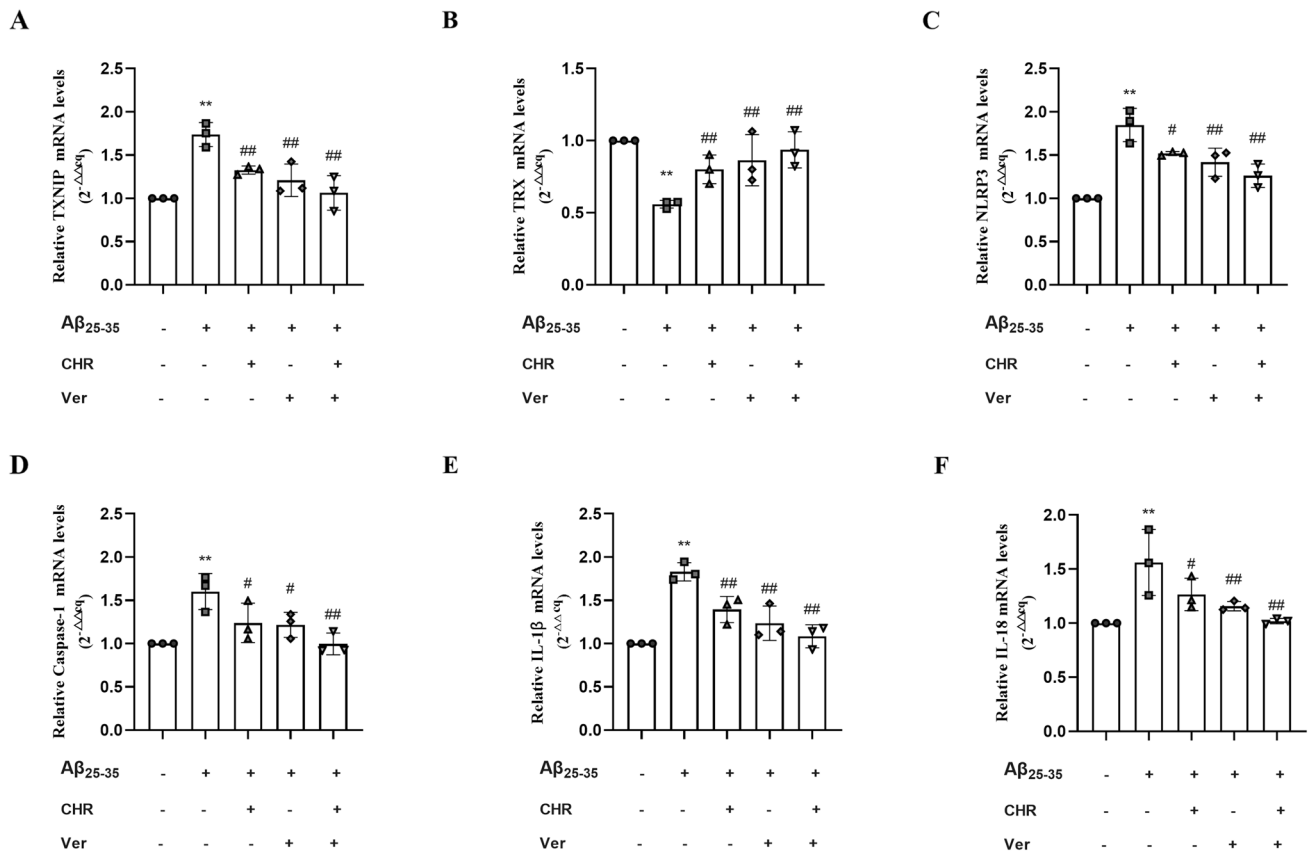
Fig. 9 Effect of CHR on the mRNA level of TXNIP, TRX, NLRP3, Caspase-1, IL-1β and IL-18 in the AD cells. **A** TXNIP mRNA. **B** TRX mRNA. **C** NLRP3 mRNA. **D** Caspase-1 mRNA. **E** IL-1β mRNA. **F** IL-18 mRNA. Data are expressed as mean ± SD. **$P < 0.01$, vs. Control group; #$P < 0.05$, ##$P < 0.01$, vs. Aβ25-35 group

Table 2 Docking results of CHR with the TXNIP

Chemicals	Vina score	Cavity score	Center (x, y, z)	Size (x, y, z)	Amino acid residues
Ver	−5.7	555	17, 39, −8	27, 27, 27	**LEU78, GLU79, ASP80, GLN81, ILE90, ARG92, ASN95, LYS96, TYR97, GLU98,** LYS100
CHR	−6.6	555	17, 39, −8	19, 19, 19	**LEU78, GLU79, ASP80, GLN81, ILE90, ARG92, ASN95, LYS96, TYR97, GLU98**

The bold represents the same amino acid residues
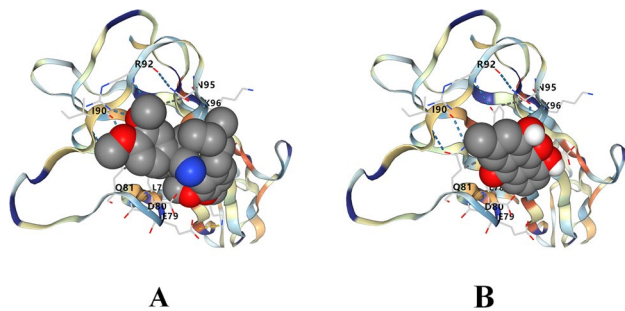
Fig. 10 The docking pictures of Ver or CHR with TXNIP. **A** Ver-TXNP, **B** CHR-TXNIP

inhibiting downstream NLRP3 activation and the release of IL-1β and IL-18, thus exerting neuroprotective effects against AD (Fig. 11). Finally, we used molecular docking to verify the experimental results. The results showed that the Vina score of CHR and TXNIP target was -6.6, and its affinity was better than that of Ver (-5.7), indicating that the mechanism of CHR in the treatment of AD was similar to that of verapamil, both acting on TXNIP. These results suggest that CHR can play a neuroprotective role in AD by inhibiting TXNIP-mediated oxidative stress and inflammatory injury.
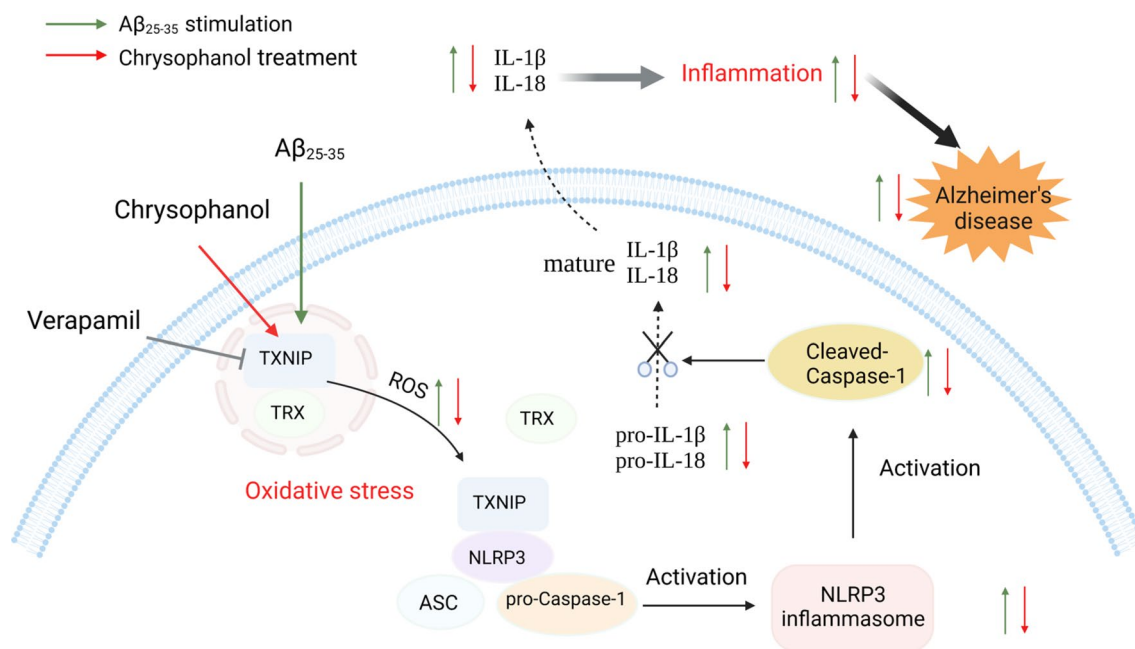
Fig. 11 Mechanism diagram of CHR exerting neuroprotective effect by regulating ROS/TXNIP/NLRP3 signaling pathway

Conclusion

In this study, we have proved that CHR can significantly improve $A\beta_{25-35}$-induced cognitive damage and hippocampal neuron damage, reduce cell apoptosis, and play a neuroprotective role by inhibiting oxidative stress and neuroinflammation in AD rats and PC12 cell models. Its mechanism may be related to ROS/TXNIP/NLRP3 signal pathway, which provides an experimental basis for the clinical treatment of AD. However, this article has some shortcomings, mainly in in vivo experiments, single-dose of CHR was used to explore the mechanism of AD. In the future experimental design, we will design a positive control drug group and more than two test concentrations of CHR.

References

Ashrafian H, Zadeh EH, Khan RH (2021) Review on Alzheimer's disease: inhibition of amyloid beta and tau tangle formation. Int J Biol Macromol 167:382–394

Bharti V, Tan H, Zhou H, Wang JF (2019) Txnip mediates glucocorticoid-activated NLRP3 inflammatory signaling in mouse microglia. Neurochem Int 131:104564

Cai B, Ye S, Wang Y, Hua RP, Wang TT, Lix LJ, Jiang AJ, Shen GM (2018) Protective effects of genistein on $A\beta_{25-35}$-induced PC12 cell injury via regulating CaM-CaMKIV signaling pathway. Zhongguo Zhong Yao Za Zhi 43:571–576

Chae U, Min JS, Lee H, Song KS, Lee HS, Lee HJ, Lee SR, Lee DS (2017a) Chrysophanol suppresses pro-inflammatory response in microglia via regulation of Drp1-dependent mitochondrial fission. Immunopharmacol Immunotoxicol 39:268–275

Chae U, Min JS, Leem HH, Lee HS, Lee HJ, Lee SR, Lee DS (2017b) Chrysophanol suppressed glutamate-induced hippocampal neuronal cell death via regulation of dynamin-related protein 1-dependent mitochondrial fission. Pharmacology 100:153–160

Chen Q, He H, Luo S, Xiong L, Li P (2014) A novel GC-MS method for determination of chrysophanol in rat plasma and tissues: Application to the pharmacokinetics, tissue distribution and

plasma protein binding studies. J Chromatogr B Analyt Technol Biomed Life Sci 973c:76–83

Chen J, Chen J, Cheng Y, Fu Y, Zhao H, Tang M, Zhao H, Lin N, Shi X, Lei Y, Wang S, Huang L, Wu W, Tan J (2020) Mesenchymal stem cell-derived exosomes protect beta cells against hypoxia-induced apoptosis via miR-21 by alleviating ER stress and inhibiting p38 MAPK phosphorylation. Stem Cell Res Ther 11:97

Cui WH, Zhang HH, Qu ZM, Wang Z, Zhang DJ, Wang S (2022) Effects of chrysophanol on hippocampal damage and mitochondrial autophagy in mice with cerebral ischemia reperfusion. Int J Neurosci 132:613–620

Dai L, Zhu L, Ma S, Liu J, Zhang M, Li J, Luo Y, Zhou X, Chen Q, Wang L, Huang Y, Chen Y (2022) Berberine alleviates NLRP3 inflammasome induced endothelial junction dysfunction through Ca^{2+} signaling in inflammatory vascular injury. Phytomedicine 101:154131

Domingues A, Jolibois J, Marquet de Rougé P, Nivet-Antoine V (2021) The emerging role of TXNIP in ischemic and cardiovascular diseases; a novel marker and therapeutic target. Int J Mol Sci 22:1693

Du J, Wang Y, Tu Y, Guo Y, Sun X, Xu X, Liu X, Wang L, Qin X, Zhu M, Song E (2020) A prodrug of epigallocatechin-3-gallate alleviates high glucose-induced pro-angiogenic factor production by inhibiting the ROS/TXNIP/NLRP3 inflammasome axis in retinal Müller cells. Exp Eye Res 196:108065

Gao J, He H, Jiang W, Chang X, Zhu L, Luo F, Zhou R, Ma C, Yan T (2015) Salidroside ameliorates cognitive impairment in a d-galactose-induced rat model of Alzheimer's disease. Behav Brain Res 293:27–33

Ge X, Wang Y, Yu S, Cao X, Chen Y, Cheng Q, Ding F (2021) Anti-inflammatory activity of a polypeptide fraction from achyranthes bidentate in Amyloid β oligomers induced model of Alzheimer's disease. Front Pharmacol 12:716177

Gu M, Zhou Y, Liao N, Wei Q, Bai Z, Bao N, Zhu Y, Zhang H, Gao L, Cheng X (2022) Chrysophanol, a main anthraquinone from *Rheum palmatum L.* (rhubarb), protects against renal fibrosis by suppressing NKD2/NF-κB pathway. Phytomedicine 105:154381

Han Y, Xu X, Tang C, Gao P, Chen X, Xiong X, Yang M, Yang S, Zhu X, Yuan S, Liu F, Xiao L, Kanwar YS, Sun L (2018) Reactive oxygen species promote tubular injury in diabetic nephropathy: the role of the mitochondrial ros-txnip-nlrp3 biological axis. Redox Biol 16:32–46

Insel PS, Donohue MC, Berron D, Hansson O, Mattsson-Carlgren N (2021) Time between milestone events in the Alzheimer's disease amyloid cascade. Neuroimage 227:117676

Ismael S, Wajidunnisam, Sakata K, McDonald MP, Liao FF, Ishrat T (2021) ER stress associated TXNIP-NLRP3 inflammasome activation in hippocampus of human Alzheimer's disease. Neurochem Int 148:105104

Ismael S, Patrick D, Salman M, Parveen A, Stanfill AG, Ishrat T (2022) Verapamil inhibits TXNIP-NLRP3 inflammasome activation and preserves functional recovery after intracerebral hemorrhage in mice. Neurochem Int 161:105423

Ju Y, Tam KY (2022) Pathological mechanisms and therapeutic strategies for Alzheimer's disease. Neural Regen Res 17:543–549

Kang L, Si L, Rao J, Li D, Wu Y, Wu S, Wu M, He S, Zhu W, Wu Y, Xu J, Li G, Huang J (2017) Polygoni multiflori radix derived anthraquinones alter bile acid disposition in sandwich-cultured rat hepatocytes. Toxicol in Vitro 40:313–323

Kang R, Li R, Dai P, Li Z, Li Y, Li C (2019) Deoxynivalenol induced apoptosis and inflammation of IPEC-J2 cells by promoting ROS production. Environ Pollut 251:689–698

Kelley N, Jeltema D, Duan Y, He Y (2019) The NLRP3 inflammasome: an overview of mechanisms of activation and regulation. Int J Mol Sci 20:3328

Khan S, Barve KH, Kumar MS (2020) Recent advancements in pathogenesis, diagnostics and treatment of Alzheimer's disease. Curr Neuropharmacol 18:1106–1125

Koka S, Xia M, Chen Y, Bhat OM, Yuan X, Boini KM, Li PL (2017) Endothelial NLRP3 inflammasome activation and arterial neointima formation associated with acid sphingomyelinase during hypercholesterolemia. Redox Biol 13:336–344

Lahooti B, Chhibber T, Bagchi S, Varahachalam SP, Jayant RD (2021) Therapeutic role of inflammasome inhibitors in neurodegenerative disorders. Brain Behav Immun 91:771–783

Li X, Chu S, Liu Y, Chen N (2019) Neuroprotective effects of anthraquinones from rhubarb in central nervous system diseases. Evid Based Complement Alternat Med 2019:3790728

Li N, Zhao T, Cao Y, Zhang H, Peng L, Wang Y, Zhou X, Wang Q, Li J, Yan M, Dong X, Zhao H, Li P (2020a) Tangshen formula attenuates diabetic kidney injury by imparting anti-pyroptotic effects via the TXNIP-NLRP3-GSDMD axis. Front Pharmacol 11:623489

Li Q, Tuo X, Li B, Deng Z, Qiu Y, Xie H (2020b) Semaglutide attenuates excessive exercise-induced myocardial injury through inhibiting oxidative stress and inflammation in rats. Life Sci 250:117531

Li X, Cheng Y, Qin Y, Gao H, Wang G, Song H, Wang Y, Cai B (2022a) Chrysophanol exerts neuroprotective effects via interfering with endoplasmic reticulum stress apoptotic pathways in cell and animal models of Alzheimer's disease. J Pharm Pharmacol 74:32–40

Li Z, Liu T, Feng Y, Tong Y, Jia Y, Wang C, Cui R, Qu K, Liu C, Zhang J (2022b) PPARγ alleviates sepsis-induced liver injury by inhibiting hepatocyte pyroptosis via inhibition of the ROS/TXNIP/NLRP3 signaling pathway. Oxid Med Cell Longev 2022:1269747

Lian D, Dai L, Xie Z, Zhou X, Liu X, Zhang Y, Huang Y, Chen Y (2018) Periodontal ligament fibroblasts migration injury via ROS/TXNIP/Nlrp3 inflammasome pathway with Porphyromonas gingivalis lipopolysaccharide. Mol Immunol 103:209–219

Lim W, An Y, Yang C, Bazer FW, Song G (2018) Chrysophanol induces cell death and inhibits invasiveness via mitochondrial calcium overload in ovarian cancer cells. J Cell Biochem 119:10216–10227

Lin F, Zhang C, Chen X, Song E, Sun S, Chen M, Pan T, Deng X (2015) Chrysophanol affords neuroprotection against microglial activation and free radical-mediated oxidative damage in BV2 murine microglia. Int J Clin Exp Med 8:3447–3455

Liu W, Gu J, Qi J, Zeng XN, Ji J, Chen ZZ, Sun XL (2015) Lentinan exerts synergistic apoptotic effects with paclitaxel in A549 cells via activating ROS-TXNIP-NLRP3 inflammasome. J Cell Mol Med 19:1949–1955

Liu X, Zhang X, Chen J, Song D, Zhang C, Chen R, Xu R, Jiang W, Li L (2022a) Chrysophanol facilitates long-term neurological recovery through limiting microglia-mediated neuroinflammation after ischemic stroke in mice. Int Immunopharmacol 112:109220

Liu Y, Shang W, Liu H, Hui H, Wu J, Zhang W, Gao P, Guo K, Guo Y, Tian J (2022b) Biomimetic manganese-eumelanin nanocomposites for combined hyperthermia-immunotherapy against prostate cancer. J Nanobiotechnol 20:48

Liu Y, Yang X, Gan J, Chen S, Xiao ZX, Cao Y (2022c) CB-Dock2: improved protein-ligand blind docking by integrating cavity detection, docking and homologous template fitting. Nucleic Acids Res 50:W159-164

Lu L, Lu Q, Chen W, Li J, Li C, Zheng Z (2018) Vitamin D(3) protects against diabetic retinopathy by inhibiting high-glucose-induced activation of the ROS/TXNIP/NLRP3 inflammasome pathway. J Diabetes Res 2018:8193523

Martínez MA, Rodríguez JL, Lopez-Torres B, Martínez M, Martínez-Larrañaga MR, Maximiliano JE, Anadón A, Ares I (2020) Use of human neuroblastoma SH-SY5Y cells to

evaluate glyphosate-induced effects on oxidative stress, neuronal development and cell death signaling pathways. Environ Int 135:105414

Melone MAB, Dato C, Paladino S, Coppola C, Trebini C, Giordana MT, Perrone L (2018) Verapamil inhibits Ser202/Thr205 phosphorylation of tau by blocking TXNIP/ROS/p38 MAPK pathway. Pharm Res 35:44

Minutoli L, Puzzolo D, Rinaldi M, Irrera N, Marini H, Arcoraci V, Bitto A, Crea G, Pisani A, Squadrito F, Trichilo V, Bruschetta D, Micali A, Altavilla D (2016) ROS-mediated NLRP3 inflammasome activation in brain, heart, kidney, and testis ischemia/reperfusion injury. Oxid Med Cell Longev 2016:2183026

Nasoohi S, Ismael S, Ishrat T (2018) Thioredoxin-interacting protein (TXNIP) in cerebrovascular and neurodegenerative diseases: regulation and implication. Mol Neurobiol 55:7900–7920

Polekhina G, Ascher DB, Kok SF, Beckham S, Wilce M, Waltham M (2013) Structure of the N-terminal domain of human thioredoxin-interacting protein. Acta Crystallogr D Biol Crystallogr 69:333–344

Popović N, Morales-Delgado N, Vidal Mena D, Alonso A, Pascual Martínez M, Caballero Bleda M, Popović M (2020) Verapamil and Alzheimer's disease: past, present, and future. Front Pharmacol 11:562

Se Thoe E, Fauzi A, Tang YQ, Chamyuang S, Chia AYY (2021) A review on advances of treatment modalities for Alzheimer's disease. Life Sci 276:119129

Sharma P, Srivastava P, Seth A, Tripathi PN, Banerjee AG, Shrivastava SK (2019) Comprehensive review of mechanisms of pathogenesis involved in Alzheimer's disease and potential therapeutic strategies. Prog Neurobiol 174:53–89

Shen Y, Hua L, Yeh CK, Shen L, Ying M, Zhang Z, Liu G, Li S, Chen S, Chen X, Yang X (2020) Ultrasound with microbubbles improves memory, ameliorates pathology and modulates hippocampal proteomic changes in a triple transgenic mouse model of Alzheimer's disease. Theranostics 10:11794–11819

Shi Y, Jin Y, Liu F, Jiang J, Cao J, Lu Y, Yang J (2021) Ceramide induces the apoptosis of non-small cell lung cancer cells through the Txnip/Trx1 complex. Int J Mol Med 47:85

Sreelakshmi V, Raj N, Abraham A (2017) Evaluation of the drug-like properties of kaempferol, chrysophanol and emodin and their interactions with EGFR tyrosine kinase—An in silico approach. Nat Prod Commun 12:915–920

Srivastava S, Ahmad R, Khare SK (2021) Alzheimer's disease and its treatment by different approaches: a review. Eur J Med Chem 216:113320

Su S, Wu J, Gao Y, Luo Y, Yang D, Wang P (2020) The pharmacological properties of chrysophanol, the recent advances. Biomed Pharmacother 125:110002

Sun XY, Li LJ, Dong QX, Zhu J, Huang YR, Hou SJ, Yu XL, Liu RT (2021) Rutin prevents tau pathology and neuroinflammation in a mouse model of Alzheimer's disease. J Neuroinflamm 18:131

Tsubaki H, Tooyama I, Walker DG (2020) Thioredoxin-interacting protein (TXNIP) with focus on brain and neurodegenerative diseases. Int J Mol Sci 21:9357

Wang Y, Cai B, Shao J, Wang TT, Cai RZ, Ma CJ, Han T, Du J (2016) Genistein suppresses the mitochondrial apoptotic pathway in hippocampal neurons in rats with Alzheimer's disease. Neural Regen Res 11:1153–1158

Wang W, Wu QH, Sui Y, Wang Y, Qiu X (2017) Rutin protects endothelial dysfunction by disturbing Nox4 and ROS-sensitive NLRP3 inflammasome. Biomed Pharmacother 86:32–40

Wang DS, Yan LY, Yang DZ, Lyu Y, Fang LH, Wang SB, Du GH (2020) Formononetin ameliorates myocardial ischemia/reperfusion injury in rats by suppressing the ROS-TXNIP-NLRP3 pathway. Biochem Biophys Res Commun 525:759–766

Wei H, Gao Z, Zheng L, Zhang C, Liu Z, Yang Y, Teng H, Hou L, Yin Y, Zou X (2017) Protective effects of fucoidan on Aβ$_{25-35}$ and d-Gal-induced neurotoxicity in PC12 cells and d-Gal-induced cognitive dysfunction in mice. Mar Drugs 15:77

Xia P, Marjan M, Liu Z, Zhou W, Zhang Q, Cheng C, Zhao M, Tao Y, Wang Z, Ye Z (2022) Chrysophanol postconditioning attenuated cerebral ischemia-reperfusion injury induced NLRP3-related pyroptosis in a TRAF6-dependent manner. Exp Neurol 357:114197

Xie L, Tang H, Song J, Long J, Zhang L, Li X (2019) Chrysophanol: a review of its pharmacology, toxicity and pharmacokinetics. J Pharm Pharmacol 71:1475–1487

Xu L, Yu Y, Sang R, Li J, Ge B, Zhang X (2018) Protective effects of taraxasterol against ethanol-induced liver injury by regulating CYP2E1/Nrf2/HO-1 and NF-κB signaling pathways in mice. Oxid Med Cell Longev 2018:8284107

Xuan WT, Wang H, Zhou P, Ye T, Gao HW, Ye S, Wang JH, Chen ML, Song H, Wang Y, Cai B (2020) Berberine ameliorates rats model of combined Alzheimer's disease and type 2 diabetes mellitus via the suppression of endoplasmic reticulum stress. 3 Biotech 10:359

Yang X, Zhi J, Leng H, Chen Y, Gao H, Ma J, Ji J, Hu Q (2021) The piperine derivative HJ105 inhibits Aβ(1–42)-induced neuroinflammation and oxidative damage via the Keap1-Nrf2-TXNIP axis. Phytomedicine 87:153571

Yang Y, Zhang D, Wu L, Zhang J, Wu D, Li X, Zhi F, Yang G, Kong X, Hong J, Zhao Y, Liu J, Shi Z, Ma X (2022) Electroacupuncture inhibits the corneal ROS/TXNIP/NLRP3 signaling pathway in a rat model of dry eye syndrome. Acupunct Med 40:78–88

Ye X, Zuo D, Yu L, Zhang L, Tang J, Cui C, Bao L, Zan K, Zhang Z, Yang X, Chen H, Tang H, Zu J, Shi H, Cui G (2017) ROS/TXNIP pathway contributes to thrombin induced NLRP3 inflammasome activation and cell apoptosis in microglia. Biochem Biophys Res Commun 485:499–505

Ye S, Cai B, Zhou P, Wang G, Gao H, Hua R, You L, Yao Y, Wang Y, Shen G (2020a) Huang-Pu-Tong-Qiao formula ameliorates tau phosphorylation by inhibiting the CaM-CaMKIV pathway. Evid Based Complement Alternat Med 2020:8956071

Ye T, Gao HW, Xuan WT, Ye S, Zhou P, Li XQ, Wang Y, Song H, Liu YY, Cai B (2020b) The regulating mechanism of chrysophanol on protein level of CaM-CaMKIV to protect PC12 cells against Aβ(25–35)-induced damage. Drug Des Devel Ther 14:2715–2723

Ye T, Li X, Zhou P, Ye S, Gao H, Hua R, Ma J, Wang Y, Cai B (2020c) Chrysophanol improves memory ability of d-galactose and Aβ(25–35) treated rat correlating with inhibiting tau hyperphosphorylation and the CaM-CaMKIV signal pathway in hippocampus. 3 Biotech 10:111

Yusuf MA, Singh BN, Sudheer S, Kharwar RN, Siddiqui S, Abdel-Azeem AM, Fernandes Fraceto L, Dashora K, Gupta VK (2019) Chrysophanol: a natural anthraquinone with multifaceted biotherapeutic Potential. Biomolecules 9:68

Zhang H, Guo Z, Wu N, Xu W, Han L, Li N, Han Y (2012) Two novel naphthalene glucosides and an anthraquinone isolated from Rumex dentatus and their antiproliferation activities in four cell lines. Molecules 17:843–850

Zhang N, Zhang X, Liu X, Wang H, Xue J, Yu J, Kang N, Wang X (2014) Chrysophanol inhibits NALP3 inflammasome activation and ameliorates cerebral ischemia/reperfusion in mice. Mediat Inflamm 2014:370530

Zhao Y, Zeng CY, Li XH, Yang TT, Kuang X, Du JR (2020) Klotho overexpression improves amyloid-β clearance and cognition in the APP/PS1 mouse model of Alzheimer's disease. Aging Cell 19:e13239

Zhao X, Qiao D, Guan D, Wang K, Cui Y (2022) Chrysophanol ameliorates hemin-induced oxidative stress and endoplasmic reticulum stress by regulating microRNA-320-5p/Wnt3a pathway in HT22 cells. Oxid Med Cell Longev 2022:9399658